Available online at www.sciencedirect.com
SCIENCE DIRECT®
Int. J. Electron. Commun. (AEÜ) 59 (2005) 147–156
International Journal AEÜ of Electronics and Communications
www.elsevier.de/aeue

Frequency selective signal extrapolation with applications to error concealment in image communication

André Kaup[a,*], Katrin Meisinger[a], Til Aach[b]

[a] *Chair of Multimedia Communications and Signal Processing, University of Erlangen-Nuremberg, Cauerstr. 7, 91058 Erlangen, Germany*
[b] *Institute for Image Processing and Computer Vision, RWTH Aachen University, 52056 Aachen, Germany*

Received 16 March 2005

Dedicated to Prof. Lüke on the occasion of his 70th birthday

Abstract

Signal extrapolation is an important topic in image communication where it can be used for various prediction purposes such as concealment of image data corrupted by transmission errors. This contribution outlines a method for extrapolating a signal beyond a limited number of known samples. The known signal samples are approximated by a set of basis functions which are defined over an area covering known as well as unknown samples. By minimizing a suitable error criterion and successively selecting the most dominant basis functions, a non band-limited signal extrapolation can be obtained. It is shown that this extrapolation can successfully be used for concealment of transmission errors in video communication as well as elimination of defective pixels in X-ray imaging.

Keywords: Signal extrapolation; Error concealment; Image and video communication; X-ray imaging

1. Introduction

Extending a signal beyond a limited number of known samples is commonly referred to as signal extrapolation. In image and video communication, signal extrapolation is an important issue in various applications. The problem of concealing corrupted image data, for example, can be seen as an extrapolation of the surrounding available image data into the missing area. In image coding, spatial prediction of a signal is applied in order to increase coding efficiency. This prediction step can also be interpreted as extrapolation of the known signal.

Approaches for signal extrapolation by spectral analysis are known from digital signal processing. The observed time-limited signal can be modeled as a multiplication of the unknown signal by a time-limited binary window function. In the frequency domain, the convolution of the unknown signal spectrum with the window spectrum leads to a blurred and spread spectrum of the observed signal. Our objective is to eliminate the influence of the known window spectrum by spectral analysis, thus extrapolating the signal beyond the known samples.

Several iterative approaches are known for Fourier based spectral analysis. The techniques in [1,2] treat the extrapolation of time-windowed signals with known limited bandwidth. The spectrum of the observed windowed signal is first limited to the known band and then transformed to the time domain, yielding a signal which is extrapolated beyond the known samples. Band limitation, however, also alters the

* Corresponding author.
E-mail addresses: kaup@LNT.de (A. Kaup), meisinger@LNT.de (K. Meisinger), til.aach@lfm.rwth-aachen.de (T. Aach).

1434-8411/$ - see front matter © 2005 Elsevier GmbH. All rights reserved.
doi:10.1016/j.aeue.2005.03.015

samples within the time window. After replacing the altered samples by the known window-internal samples, the signal is transformed again into the frequency domain, where band limitation is enforced. The extrapolation is obtained by iterating this procedure. In [2] spectral components are additionally eliminated which are below an adaptive threshold. However, because of the band limitation the signal decays rapidly in the time domain beyond the known samples in the extrapolated area. Therefore the approach is not suitable for applications where the emphasis is placed on extrapolation into larger areas.

In [3], an iterative extrapolation approach for region oriented image analysis is described which in each step selects the spectral component with largest magnitude. The undesirable signal decay in the extrapolated area is avoided due to signal expansion restricted to a small subset of dominant spectral coefficients. As the previous approaches the technique alternates in each iteration between signal and frequency domain, and hence has a high computational complexity. This repetitive transformation is avoided by the proposal in [4,5] which, exploiting Parseval's theorem, estimates the spectrum completely in the frequency domain. Here the application is modelling the human sense of hearing by a high resolution spectral analysis. In [5] some examples for a 2D generalization of this spectrum estimation are given with application to image extrapolation.

Extrapolation may also occur as a by-product in object based transform coding. In [6] the texture of an arbitrarily shaped object is approximated successively and represented by a linear combination of a few weighted suitable basis functions defined over a circumscribing rectangle. Then the texture is cut to the shape of the object by discarding the extrapolated areas. This approach does not rely on the convolution theorem, and is thus applicable to transforms other than the DFT, such as the DCT or DHT.

The same principle has been used in [7] for prediction of uncovered background in object-based video coding using spatial extrapolation. Here, the surrounding known background signal is successively approximated thereby yielding a prediction for the uncovered area.

Error concealment is the extrapolation of data into the missing area. Data losses can be caused in mobile video communication by transmission errors. Depending on the coding scheme, the transmission errors have different effects on the received image. In case of block coding like JPEG, errors cause block losses.

Wang et al. [8] assume that the image content is changing smoothly. This standard approach tries to restore the transition across the block boundary as smoothly as possible. The sequential method of [9] predicts each pixel from the available next neighbors. The lost block is reconstructed pixel by pixel from eight directions and given by a weighted linear combination of these reconstructed blocks thus requiring an extensive computational load. The extrapolation performance of error concealment techniques [8–12] are mostly heuristic and allow only the reconstruction of monotonous areas and edges. Moreover they allow only the satisfactory concealment of small missing areas.

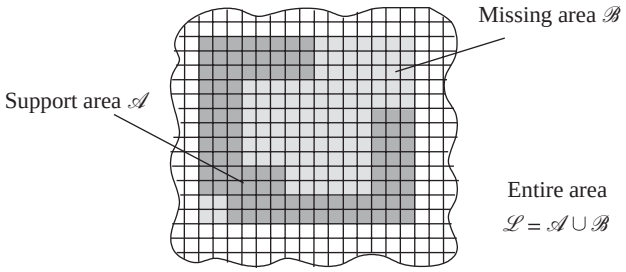

Fig. 1. The principle of extrapolation: the missing area $\mathcal{B}$ (light gray) is extrapolated from the approximated support area $\mathcal{A}$ (dark gray).

We seek to overcome these disadvantages by the convincing extrapolation properties of the frequency selective extrapolation algorithm derived in [6]. In Section 2 we introduce a slightly generalized principle of this extrapolation algorithm and then specify it for DFT basis functions. In Section 3 we apply the extrapolation technique to the concealment of erroneous image data, followed by some conclusions in Section 4.

2. Signal extrapolation

We consider the image region $\mathcal{L}$ shown shaded in Fig. 1. Our aim is to estimate the missing signal samples in the area $\mathcal{B}$ from the given signal samples in the support area $\mathcal{A}$ by extrapolation. The extrapolation principle works as follows: the signal samples in the support area $\mathcal{A}$ are approximated by a weighted linear combination of basis functions which are defined over the entire area $\mathcal{L}$. Therefore, each approximation over the support area $\mathcal{A}$ at the same time provides an estimation of the missing samples in $\mathcal{B}$. Note that $\mathcal{A}$ as well as $\mathcal{B}$ can be arbitrarily shaped, subject to the constraint that their union $\mathcal{L}$ forms a circumscribing rectangle.

In order to extrapolate data we take advantage of the extrapolating properties of basis functions. In general periodic functions are suited because they are able to extend the signal periodically. In contrast to this, functions of limited extent, such as polynomials or wavelets, are not suited because they lack the extrapolation ability if the missing area becomes larger. Therefore, periodic functions like the DCT or DFT are suited for the extrapolation of image signals. Using DFT basis functions is addressed in detail in Section 2.2. First, we will derive the general principle of the extrapolation algorithm with real valued signals and arbitrary real valued basis functions.

2.1. Extrapolation principle

The values of the samples in the support area $\mathcal{A}$ are denoted by $f[m, n]$, where m indicates the row and n the col-

umn index. A parametric model $g[m,n]$ shall approximate the signal within the support area by a linear combination of basis functions $\varphi_{k,l}[m,n]$ defined on the entire area $\mathscr{L}$ weighted by expansion coefficients $c_{k,l}$

$$g[m,n] = \sum_{(k,l)\in\mathscr{K}} c_{k,l}\,\varphi_{k,l}[m,n] \tag{1}$$

with $\mathscr{K}$ denoting the set of basis functions used. The number of available basis functions equals the number of samples in the entire area $\mathscr{L}$.

In order to determine the expansion coefficients, we minimize a weighted error criterion between the original signal and the parametric model evaluated with respect to the support area. The weighting function $w[m,n]$ has amplitudes $\rho[m,n]$ in the support area and is zero elsewhere

$$w[m,n] = \begin{cases} \rho[m,n], & (m,n)\in\mathscr{A}, \\ 0, & (m,n)\in\mathscr{B}. \end{cases} \tag{2}$$

The following weighted error criterion is minimized during the approximation with respect to the support area

$$E_{\mathscr{A}} = \sum_{(m,n)\in\mathscr{L}} w[m,n](f[m,n]-g[m,n])^2. \tag{3}$$

The weighting function allows us to emphasize subareas in $\mathscr{A}$ which are closer to the missing samples and thus more important for the extrapolation.

The weighted error criterion is minimized by taking the derivative with respect to the unknown coefficients and setting it to zero

$$\frac{\partial E_{\mathscr{A}}}{\partial c_{k,l}} = 0. \tag{4}$$

However, this minimization procedure does not lead to a unique solution because we have an underdetermined problem. The reason is that the number of basis functions equals the number of samples in $\mathscr{L}$ which is larger than the number of given signal samples in $\mathscr{A}$. To overcome this problem, we use the technique of successive approximation. This iterative procedure approximates the signal within the support area successively subject to an error energy constraint, leading to two steps per iteration: First, a suitable basis function is selected as described in Section 2.1.2. Secondly, the respective expansion coefficient is optimally estimated as derived in Section 2.1.1. Hence, we describe the support area by a few dominant features in terms of weighted basis functions.

2.1.1. Coefficient update

Let us assume that at any step v the parametric model $g^{(v)}[m,n]$ approximating the signal in the support area is available as

$$g^{(v)}[m,n] = \sum_{(k,l)\in\mathscr{K}_v} c_{k,l}^{(v)}\,\varphi_{k,l}[m,n] \tag{5}$$

with $\mathscr{K}_v$ denoting the set of basis functions used in this step. In the beginning, $\mathscr{K}_v$ will be empty for $v=0$ and the parametric model $g^{(0)}[m,n]$ is zero. With the window function

$$b[m,n] = \begin{cases} 1, & (m,n)\in\mathscr{A}, \\ 0, & (m,n)\in\mathscr{B} \end{cases} \tag{6}$$

we can express the residual error signal in the support area $(m,n)\in\mathscr{A}$ at any iteration v by

$$r^{(v)}[m,n] = \Big(f[m,n]-g^{(v)}[m,n]\Big)\cdot b[m,n]. \tag{7}$$

The residual error in the support area is further approximated by a weighted suitable basis function $\varphi_{u,v}[m,n]$, leading to the reduced error signal

$$r^{(v+1)}[m,n] = \Big(r^{(v)}[m,n]-\Delta c\varphi_{u,v}[m,n]\Big)\cdot b[m,n]. \tag{8}$$

In order to obtain Δc, the weighted residual error energy

$$E_{\mathscr{A}}^{(v+1)} = \sum_{(m,n)\in\mathscr{L}} w[m,n]\Big(r^{(v)}[m,n] - \Delta c\varphi_{u,v}[m,n]\Big)^2 \tag{9}$$

is minimized with respect to Δc which yields $b[m,n]w[m,n]=w[m,n]$

$$\Delta c = \frac{\sum_{(m,n)\in\mathscr{L}} w[m,n]r^{(v)}[m,n]\varphi_{u,v}[m,n]}{\sum_{(m,n)\in\mathscr{L}} w[m,n]\varphi_{u,v}^2[m,n]}. \tag{10}$$

The expansion coefficient $c_{u,v}^{(v+1)}$ is then updated by

$$c_{u,v}^{(v+1)} = c_{u,v}^{(v)} + \Delta c \tag{11}$$

and the index (u,v) is included in the set of used basis functions

$$\mathscr{K}_{v+1} = \mathscr{K}_v \cup \{u,v\} \quad \text{if } (u,v)\notin\mathscr{K}_v. \tag{12}$$

2.1.2. Selection of suitable basis functions

The question not tackled so far is how to select a suitable basis function $\varphi_{u,v}[m,n]$. We seek to select that basis function $\varphi_{u,v}[m,n]$ which minimizes our specified error criterion. Therefore, we calculate the weighted residual error energy from iteration v to $v+1$, taking into account that the residuum $r^{(v)}[m,n]$ is orthogonal to the selected basis function

$$\begin{aligned} &\sum_{(m,n)\in\mathscr{L}} w[m,n]\Big(r^{(v+1)}[m,n]\Big)^2 \\ &\quad = \sum_{(m,n)\in\mathscr{L}} w[m,n]\Big(r^{(v)}[m,n]\Big)^2 \\ &\qquad - \sum_{(m,n)\in\mathscr{L}} w[m,n](\Delta c\varphi_{u,v}[m,n])^2. \end{aligned} \tag{13}$$

More precisely, we select that basis function with index (u, v) which results in a maximal decrease of the error criterion. With help of Eq. (10) we obtain

$$\Delta E_{\mathscr{A}}^{(v)} = \Delta c^2 \sum_{(m,n)\in\mathscr{L}} w[m,n](\varphi_{u,v}[m,n])^2 = \frac{\left(\sum_{(m,n)\in\mathscr{L}} w[m,n] r^{(v)}[m,n]\varphi_{u,v}[m,n]\right)^2}{\sum_{(m,n)\in\mathscr{L}} w[m,n](\varphi_{u,v}[m,n])^2} \quad (14)$$

and select the basis function according to

$$(u, v) = \arg\max_{(k,l)} \Delta E_{\mathscr{A}}^{(v)}. \quad (15)$$

Eq. (13) shows further, that convergence of the algorithm is assured since the error energy is definitely reduced in each step.

The algorithm is initialized by

$$g^{(0)}[m,n] = 0 \quad (16)$$

and terminates when the error energy reduction $\Delta E_{\mathscr{A}}^{(v)}$ drops below a prespecified threshold $\Delta E_{\min}$.

The successive approximation procedure results in a parametric model $g[m, n]$ given in the support area $\mathscr{A}$. Hence, each approximation provides at the same time a signal extrapolation in the entire area $\mathscr{L}$ and the signal missing in area $\mathscr{B}$ is obtained by cutting it out of the parametric model.

The weighting function should emphasize regions which are closer to the missing area and thus more important for the extrapolation. Different weighting functions $w[m, n]$ are specified for isolated and consecutive block losses in Section 3.1.

2.2. Frequency selective extrapolation using 2D DFT basis functions

It has already been mentioned that periodic basis functions, such as those of the DCT and the DFT, are suited for extrapolation of image signals. Two-dimensional DCT basis functions contain only horizontal and vertical structures whereas the DFT has also diagonal basis images being therefore better suited for the signal extrapolation [13].

In the following we will apply the principle of selective extrapolation to the special case of two-dimensional DFT basis functions.

2.2.1. Frequency selective extrapolation of 2D signals

Using two-dimensional DFT basis functions

$$\varphi_{k,l}[m,n] = e^{j2\pi/Mmk} e^{j2\pi/Nnl} \quad (17)$$

we obtain for the parametric model in iteration v

$$g^{(v)}[m,n] = \frac{1}{MN} \sum_{(k,l)\in\mathscr{K}_v} c_{k,l}^{(v)} \varphi_{k,l}[m,n] = \frac{1}{MN} \sum_{(k,l)\in\mathscr{K}_v} G^{(v)}[k,l] e^{j2\pi/Mmk} e^{j2\pi/Nnl} \quad (18)$$

with M being the number of rows and N the number of columns. Obviously, the expansion coefficient becomes the DFT coefficient

$$c_{k,l}^{(v)} = G^{(v)}[k,l]. \quad (19)$$

For these complex basis functions, we minimize by

$$\frac{\partial E_{\mathscr{A}}}{\partial \Delta c^*} = 0. \quad (20)$$

We now derive some algorithmical simplifications. In Eqs. (10) and (14) the term $w[m, n]\ r^{(v)}[m, n]$ appears. For the sake of simplicity, we introduce the new variable $r_w^{(v)}[m, n]$

$$r_w^{(v)}[m,n] = w[m,n] r^{(v)}[m,n] \quad (21)$$

and rewrite Eqs. (10) and (14) in case of using DFT basis functions accordingly to

$$\Delta c = MN \frac{\sum_{(m,n)\in\mathscr{L}} r_w^{(v)}[m,n]\varphi_{u,v}^*[m,n]}{\sum_{(m,n)\in\mathscr{L}} w[m,n]\varphi_{u,v}[m,n]\varphi_{u,v}^*[m,n]} \quad (22)$$

$$\Delta E_{\mathscr{A}}^{(v)} = \frac{\left(\sum_{(m,n)\in\mathscr{L}} r_w^{(v)}[m,n]\varphi_{u,v}^*[m,n]\right)^2}{\left(\sum_{(m,n)\in\mathscr{L}} w[m,n]\varphi_{u,v}^*[m,n]\varphi_{u,v}[m,n]\right)^2} \times \sum_{(m,n)\in\mathscr{L}} w[m,n]\varphi_{u,v}^2[m,n]. \quad (23)$$

Thus, instead of inserting $r^{(v)}[m, n]$ and weighting it, we already insert the weighted residual error. Subsequently, we have to adapt Eq. (8) for the computation of the residual error in the next iteration $v + 1$, too

$$w[m,n] r^{(v+1)}[m,n] = r_w^{(v+1)}[m,n] = r_w^{(v)}[m,n] - \frac{1}{MN} \times \Delta c \varphi_{u,v}[m,n] w[m,n].$$

The evaluation of the sums in Eqs. (22) and (23) is computationally expensive. Using DFT basis functions allows us to express all equations in the frequency domain enabling an efficient implementation of the extrapolation algorithm. The multiplication of the weighting function with the complex exponential $\varphi_{u,v}[m, n]$ is equivalent to a shift of its DFT by u and v

$$\sum_{(m,n)\in\mathscr{L}} w[m,n]\varphi_{u,v}[m,n]\varphi_{k,l}[m,n] = W^*[k-u, l-v].$$

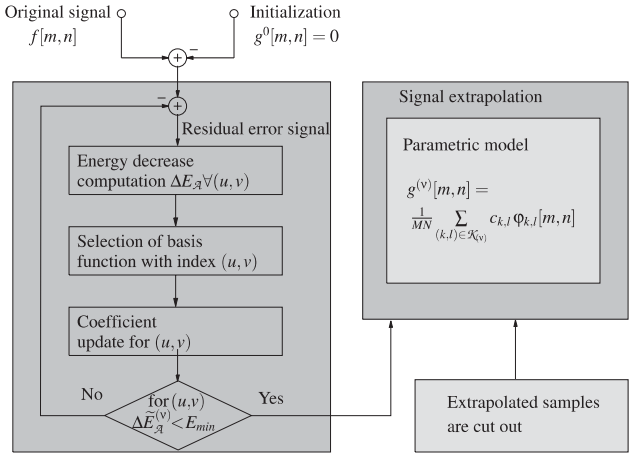

Fig. 2. Flow graph explaining the extrapolation algorithm.

Hence we can express the coefficient update Eq. (22) in the frequency domain as

$$\Delta c = MN\,\frac{R_w^{(v)}[u,v]}{W[0,0]} \tag{24}$$

as well as the energy decrease for the selection of the suitable basis function

$$\Delta E_{\mathcal{A}}^{(v)} = \frac{R_w^{(v)}[k,l]^2}{W[0,0]}. \tag{25}$$

Finally, the residual error signal according to Eq. (24) is

$$R_w^{(v+1)}[k,l] = R_w^{(v)}[k,l] - \frac{1}{MN}\Delta c\,W[k-u,l-v]. \tag{26}$$

The parametric model is obtained by an inverse DFT

$$g[m,n] = \mathrm{IDFT}_{M,N}\{G[k,l]\} \tag{27}$$

and the missing data samples are cut out. Since all equations are expressed in the frequency domain, there is only one DFT transform required in the beginning and an inverse DFT in the end.

The extrapolation algorithm is summarized by the flow graph in Fig. 2. The signal in the support area is approximated successively by computing one expansion coefficient per iteration requiring the following two steps. First, that basis function $\varphi_{u,v}[m,n]$ is selected which maximizes the decrease of the residual error energy. Then the respective coefficient $c_{u,v}^{(v)}$ is computed by minimizing the residual error energy. Subsequently, the residual error signal in the support area is computed and further approximated by the next coefficient. The iteration stops when the decrease of the residual error energy drops below a prespecified threshold. The parametric model is then given in the entire area and the missing samples are obtained by an inherent extrapolation.

2.2.2. Frequency selective extrapolation of image data

In the previous section we addressed the issue of extrapolating complex valued signals. Next, we turn to the extrapolation of real valued image signals using 2D DFT basis functions. For real valued signals the expansion coefficients or DFT coefficients, respectively, fulfill the following conjugate complex symmetry:

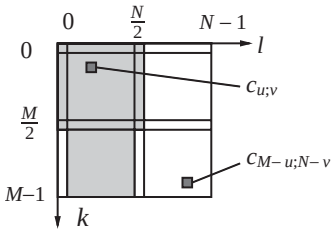

Fig. 3. Conjugate complex symmetry and search area for DFT basis functions in case of real valued image signals.

$$c_{M-k,N-l}^{(v)} = c_{k,l}^{(v)*} \text{ as well as,} \tag{28}$$

$$\varphi_{M-k,N-l}[m,n] = \varphi_{k,l}^{*}[m,n] \tag{29}$$

as illustrated in Fig. 3.

To ensure that the approximation is a real valued signal, we modify the equation for the parametric model to

$$g^{(v)}[m,n] = \frac{1}{2MN}\sum_{(k,l)\in\mathcal{K}_v}\Big(c_{k,l}^{(v)}\,\varphi_{k,l}[m,n] + c_{M-k,N-l}^{(v)}\varphi_{M-k,N-l}[m,n]\Big). \tag{30}$$

Minimizing the weighted error criterion according to

$$\frac{\partial E_{\mathcal{A}}}{\partial \Delta c} = 0 \quad \text{and} \quad \frac{\partial E_{\mathcal{A}}}{\partial \Delta c^*} = 0 \tag{31}$$

we obtain for the update equation in the frequency domain

$$\Delta c = \begin{cases} MN\,\frac{R_w^{(v)}[u,v]}{W[0,0]}, & (u,v)\in\mathcal{M} \\ 2MN\,\frac{R_w^{(v)}[u,v]W[0,0]-R_w^{*(v)}[u,v]W[2u,2v]}{W[0,0]^2-|W[2u,2v]|^2}, & \text{else} \end{cases} \tag{32}$$

with

$$\mathcal{M} = \left\{(0,0),\left(0,\frac{N}{2}\right),\left(\frac{M}{2},0\right),\left(\frac{M}{2},\frac{N}{2}\right)\right\}.$$

The case differentiation is necessary due to the definition of the parametric model in Eq. (30) and Eqs. (28) and (29). The expansion coefficients or DFT coefficients, can be updated according to

$$c_{u,v}^{(v+1)} = c_{u,v}^{(v)} + \Delta c \tag{33}$$

$$c_{M-u,N-v}^{(v+1)} = c_{M-u,N-v}^{(v)} + \Delta c^*. \tag{34}$$

The basis function with index u, v is selected which maximizes

$$\Delta E_{\mathcal{A}}^{(v)} = \begin{cases} 2\,\frac{R_w^{(v)}[k,l]^2}{W[0,0]}, & k,l \in \mathcal{M}, \\ 2\,\frac{|R_w^{(v)}[k,l]|^2 W[0,0] - \mathrm{Re}\{R_w^{(v)}[k,l]^2 W^*[2k,2l]\}}{W[0,0]^2 - |W[2k,2l]|^2}, & \text{else.} \end{cases} \quad (35)$$

However, due to the symmetry properties of the coefficients in Eq. (28) the search area for finding a suitable function can be limited to the half-plane in Fig. 3.

The modified residual error used in the approximation is given by

$$R_w^{(v+1)}[k,l] = R_w^{(v)}[k,l] - \frac{1}{2MN}(\Delta c W[k-u, l-v] + \Delta c^* W[k-(M-u), l-(N-v)]). \quad (36)$$

In contrast to Section 2.2.1, we exploit spectral symmetries of real valued image signals in order to establish the parametric model. Applying the computationally simpler concept from Section 2.2.1 to image signals is also possible. In this case the algorithm alternatingly chooses the basis function $\varphi_{u,v}[m,n]$ in iteration v and $\varphi_{M-u,N-v}[m,n]$ in $v+1$. The coefficients $c_{u,v}^{(v)}$ and $c_{M-u,N-v}^{(v+1)}$ are updated sequentially in iterations v and $v+1$. However, the residual error criterion has changed from iteration v to $v+1$ so that the coefficients $c_{u,v}^{(v)}$ and $c_{M-u,N-v}^{(v+1)}$ are not exactly conjugate complex to each other and the model function in general will be complex valued. By this, an artificial error is introduced which is avoided by the modification in Section 2.2.2.

In [5] the multiplication of the window function and the signal to be extrapolated is expressed as the convolution of the window spectrum with the signal spectrum. The window spectrum is then removed by selective spectral deconvolution. This in fact is equivalent to our approach when using DFT basis functions and restricting $w[m,n]$ in the weighted error criterion Eq. (3) to be binary valued.

3. Concealment of erroneous image data

As mentioned in the introduction error concealment of erroneous image data can be regarded as a problem of signal extrapolation. In this section, we look at the concealment of block losses and wavelet coefficients and the defect interpolation in medical images using the proposed extrapolation method. As already mentioned in Section 2, the weighting function (2) should emphasize pixels which are more important for the extrapolation over less important ones. Therefore, we choose the isotropic model [14] for $\rho[m,n]$

$$\rho[m,n] = \hat{\rho}^{\sqrt{(m-\frac{M}{2})^2+(n-\frac{N}{2})^2}}; \quad 0 < \hat{\rho} < 1 \quad (37)$$

with $\hat{\rho}$ being a prespecified constant. The influence of the weighting function decreases radial symmetrically with distance from the center of the lost area at $(M/2, N/2)$.

3.1. Block coded data

When transmitting images coded by block based techniques over error prone channels like the internet or mobile channels, the received images contain block losses in case of transmission errors. We investigate both isolated and consecutive block losses. Consecutive losses occur in case of spatial predictive coding and can be transformed into chequerboard like error patterns by block interleaving at the encoder which can be realized by the Flexible Macroblock Ordering (FMO) technique in MPEG-4/AVC [15].

Since we consider a special application in the following, we specify a model for the weighting function first.

The resulting weighting function depends also on the available support area. Fig. 4 depicts on the top the resulting weighting function for a single block loss where all surrounding blocks are available. In case of consecutive block loss which is shown on the bottom, the block next to the

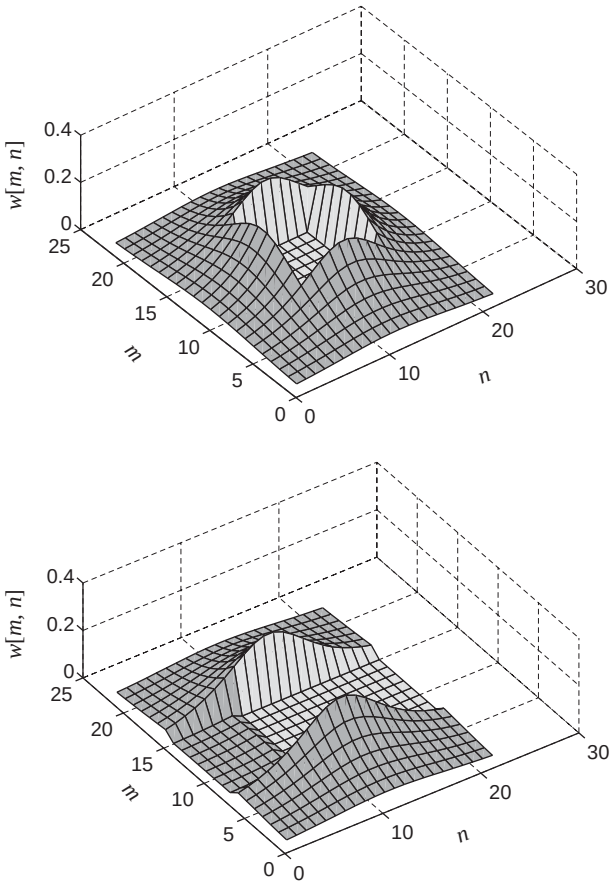

Fig. 4. Weighting function for concealment of block coded data. The light gray area denotes the missing area. Top: Isolated block loss. Bottom: Consecutive block loss.

Fig. 5. Concealment of block losses using the frequency selective extrapolation technique. Left: Isolated 16 × 16 block losses. Right: Concealed image.

missing one in raster scan order is not available. Furthermore, the previous block is an already extrapolated block weighted by 0.1 in order to include it in the concealment procedure but with limiting influence to avoid approximation error propagation.

To evaluate the ability of the algorithm to conceal errors, images with simulated block loss patterns were tested. We applied the usual macro block sizes of 16 × 16 pixels and investigated the images Lena, Peppers and Baboon containing isolated and consecutive losses.

The parameters are chosen based on the investigations done in [14], where also PSNR results with respect to the concealment techniques [8–12] are published. The support area is 13 pixels in each direction. Hence, to the resulting block of 42×42 pixels the next larger FFT size of 64×64 is applied obtained by zero padding. The input parameter $\hat{\rho}$ was set to 0.74 for the weighting function. We ran the simulations until either $\Delta E_{\mathscr{A}}$ drops below the threshold $\Delta E_{\min} = 150$ or a maximum number of 11 iterations is reached to limit computational complexity.

Fig. 5 depicts on the left-hand side the image Lena with 16 × 16 isolated losses and on the right-hand side its processed version. Obviously, the algorithm is able to extrapolate monotonous areas such as those in the background as well as edges of any direction like those along the hat. An average of 7.2 iterations per block were needed for the luminance component. In other words, approximately 7 DFT coefficient pairs were on average sufficient to extrapolate the missing area from the given support area.

Consecutive block losses are shown in Fig. 6 on the left-hand side for the image Baboon. Only parts of images are shown due to the limited space. On the right-hand side the processed image is displayed. Evidently, the algorithm extrapolates additionally noise like areas like the fur or structures like the hairs of the beard. The average number of iterations required increased slightly to 8.9 for the luminance.

Generally, in the first iteration the DC component corresponding to the color of the missing block is calculated.

Fig. 6. Concealment of block losses using the frequency selective extrapolation technique. Left: Consecutive 16 × 16 block losses. Right: Image with errors concealed.

Then, depending on the image content, the coefficients corresponding to higher frequencies are refined step by step.

A suitable weighting function improves the extrapolation results significantly. In case of concealment, the isotropic weighting function gains severable dBs in PSNR [14] with respect to a binary weighting function used in [13]. The concealment performance decreases if there are details in the support area which do not belong to the missing area. But the image content changes with increasing distance what the decaying weighting function accounts for. Further, the diagonals were overrepresented using the rectangular binary weighting function.

Fig. 7. Concealment of four packet losses in the lowpass band. Left: Lowpass with errors concealed. Right: Reconstructed image with errors concealed.

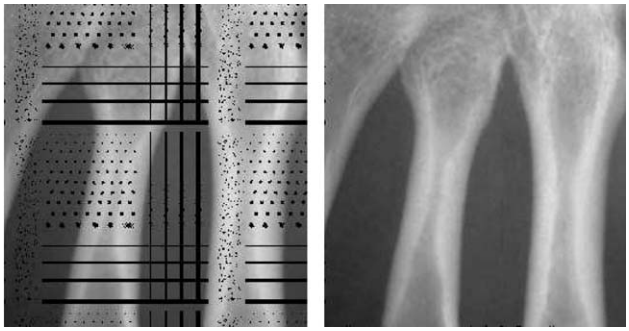

Fig. 8. Concealment of synthetically generated defective pixel sites. Left: Part of size 264 × 282 pixels of a digital radiograph with defects. Right: Image with concealed defects.

3.2. Wavelet coded data

The JPEG2000 coder as an example for a wavelet based image coder organizes wavelet coefficients in packets where a packet cannot exceed the resolution level. In case of transmission errors, the visual distortions caused by a packet loss and the related loss of wavelet coefficients are concealed by extrapolating the surrounding correctly received wavelet coefficients in the subband [16].

Fig. 7 demonstrates the concealment of wavelet coefficients. Four packet losses where applied to the lowpass signal. On the left-hand side, the concealed lowpass signal by extrapolating the lost wavelet coefficients from the surrounding coefficients is depicted using a weighting according to Eq. (37) with $\hat{\rho} = 0.45$ and maximally 4 iterations. The reconstructed image with errors concealed is shown on the right-hand side.

3.3. Defect interpolation in digital radiography

Another error concealment problem arises in clinical X-ray imaging with the advent of large-area flat panel detector systems [17,18]. Such a detector system is manufactured from amorphous silicon (a-Si), and consists of a large matrix – up to $40 \times 40\,\mathrm{cm}^2$ – of light sensitive pixels, which is made sensitive to X radiation by a coating of scintillating material. Practically, however, the current generation of these detectors contains lines and clusters of inactive pixels [18, p. 287], the sites of which are known from calibration measurements. Such defects can be interpolated from neighboring data by median filtering [18] or orientation-adaptive linear interpolation [19]. The down-side of these spatial approaches is that they are limited to defects of rather small spatial extent, and that the (quantum) noise structure in the interpolated defects may look somewhat unnatural. As an alternative, we have therefore applied the above spectral approach to radiographies with synthetically generated defects [20,21]. Fig. 8 shows on the left-hand side a part of a radiograph with synthetic defects. (To test the ability of our algorithm to cope with even large-area defects, these defects are grossly exaggerated.) The processed version is shown on the right-hand side of Fig. 8. Processing was based on the DFT applied to blocks of size 64 × 64 pixels. All known pixels within this support were weighted equally, i.e. no weighting as in Eq. (37) was used. The price to pay was that, in order to achieve good extrapolation results, the number of iterations had to be considerably increased. Also, the spectral resolution had to be doubled in each dimension by appropriate zero-padding of the signal before entering into the iteration. Details can be found in [20,21].

4. Conclusions

We presented a method for signal extrapolation. Concealment of erroneous image data can be seen as an extrapolation problem where we applied the developed algorithm successfully. Using DFT basis functions, the algorithm extrapolates fairly large missing areas by spectral analysis of a given support area. Besides, the technique is able to extend consistently signals with different properties like monotonous areas, edges as well as noise like areas. The complexity depends on the signal properties, monotonous areas require only one iteration and detailed areas more.

Future work will include the application of the promising approach to other extrapolation problems in image and video communication like intraframe prediction in video coding or image inpainting for unobtrusive removal of bothering image details such as video logos.

References

[1] Papoulis A. A new algorithm in spectral analysis and band-limited extrapolation. IEEE Trans Circuits Syst 1975;22: 735–42.
[2] Papoulis A, Chamzas C. Detection of hidden periodicities by adaptive extrapolation. IEEE Trans Acoustics Speech Signal Process 1979;27:492–500.
[3] Franke U. Regionenorientierte Bildbeschreibung-Algorithmen und Möglichkeiten. Fortschritt-Berichte VDI, Reihe 10: Informatik/Kommunikationstechnik, vol. 101, 1989.

[4] Sottek R. Modelle zur Signalverarbeitung im menschlichen Gehör. Dissertation. University RWTH Aachen, Germany, 1993.
[5] Sottek R, Illgner K, Aach T. An efficient approach to extrapolation and spectral analysis of discrete signals. Informatik-Fachberichte, 1990; 253 (ASST 90):103–8.
[6] Kaup A, Aach T. Coding of segmented images using shape-independent basis functions. IEEE Trans Image Process 1998;7:937–47.
[7] Kaup A, Aach T. Efficient prediction of uncovered background in interframe coding using spatial extrapolation. In: Proceedings of the international conference on acoustics, speech, and signal processing (ICASSP). Adelaide, Australia, April 1994. p. 501–4.
[8] Wang Y, Zhu Q-F, Shaw L. Maximally smooth image recovery in transform coding. IEEE Trans Commun 1993;41:1544–51.
[9] Xin L, Orchard MT. Novel sequential error-concealment techniques using orientation adaptive interpolation. IEEE Trans Circuits Syst Video Technol 2002;12:857–64.
[10] Sun H, Kwok W. Concealment of damaged block transform coded images using projections onto convex sets. IEEE Trans Image Process 1995;4:470–7.
[11] Alkachouh Z, Bellanger M. Fast DCT-based spatial domain interpolation of blocks in images. IEEE Trans Image Process 2000;9:729–32.
[12] Shirani S, Kossentini F, Ward R. Reconstruction of baseline JPEG coded images in error prone environments. IEEE Trans Image Process 2000;9:1292–9.
[13] Meisinger K, Kaup A. Spatial error concealment of corrupted image data using frequency selective extrapolation. In: Proceedings of the international conference on acoustics, speech, and signal processing (ICASSP). Montreal, Canada, May 2004. p. 209–12.
[14] Meisinger K, Kaup A. Minimizing a weighted error criterion for spatial error concealment of missing image data. In: Proceedings of the international conference on image processing (ICIP). Singapore, October 2004. p. 813–6.
[15] Joint video team (JVT) of ISO/IEC MPEG and ITU-T VCEG: Draft ITU-T recommendation and final draft international standard of joint video specification (ITU-T Rec. H.264—ISO/IEC 14496-10 AVC). ISO/IEC JTC1/SC29/WG11 and ITU-T SG16 Q.6, March 2003.
[16] Meisinger K, Garbas J-U, Kaup A. Error control and concealment of JPEG2000 coded image data in error prone environments. In: Proceedings of the picture coding symposium (PCS). San Francisco, December 2004.
[17] Aach T, Schiebel U, Spekowius G. Digital image acquisition and processing in medical X-ray imaging. J Electron Imaging 1999;8:7–22.
[18] Rowlands JA, Yorkston J. Flat panel detectors for digital radiography. In: Beutel J, Kundel HL, van Metter RL, editors. Handbook of medical imaging. Berlin: Springer; 2000. p. 223–328.
[19] Xu F, Liu H, Wang G, Alford BA. Comparison of adaptive linear interpolation and conventional linear interpolation for digital radiography systems. J Electron Imaging 2000;9: 22–31.
[20] Aach T, Metzler V. Defect interpolation in digital radiography—how object-oriented transform coding helps. In: Sonka M, Hanson KM, editors. Medical Imaging 2001, San Diego, USA, February 17–22 2001, SPIE, vol. 4322. p. 824–35.
[21] Aach, T. Missing data interpolation by transform-based successive approximation. Proceedings of the workshop on spectral methods and multirate signal processing (SMMSP-2001), Pula, Croatia, June 2001. p. 3–10.

André Kaup received the Dipl.-Ing. and Dr.-Ing. degrees in Electrical Engineering from Aachen University of Technology (RWTH), Germany, in 1989 and 1995, respectively. From 1989 to 1995 he was with the Institute for Communication Engineering at Aachen University of Technology, where he was responsible for industrial as well as academic research projects in the area of high resolution printed image compression, object-based image analysis and coding, and models for human perception. In 1995 he joined Siemens Corporate Technology in Munich, where he chaired European research projects in the area of very low bit rate video coding, image quality enhancement, and mobile multimedia communications. In 1999 he was appointed head of mobile applications and services, with research focussing on multimedia adaptation for heterogeneous communication networks. Since 2001 he is full professor and Head of the Chair for Multimedia Communications and Signal Processing at University of Erlangen-Nuremberg. He is member of the German Informationstechnische Gesellschaft and senior member of the IEEE. He was elected Siemens inventor of the year 1998 and is recipient of the 1999 ITG Award. From 1997 to 2001 he was also head of the German MPEG delegtion and adjunct professor at Technical University of Munich.

Katrin Meisinger received her Dipl.-Ing. degree in Electrical Engineering from the University of Erlangen-Nuremberg, Germany, in 2001. She holds currently a position as a research scientist at the Chair of Multimedia Communications and Signal Processing of the University of Erlangen-Nuremberg, Germany, where she is working towards the Dr.-Ing. degree. Her research interests include image and video signal processing with special focus on extrapolation problems as error concealment, inpainting and intra prediction.

Til Aach received his diploma and Doctoral degrees, both in EE, from Aachen University of Technology (RWTH) in 1987 and 1993, respectively. While working towards his Doctoral Degree, he was a research scientist with the Institute for Communications Engineering, Aachen University of Technology, being in charge of several projects in image analysis, 3D-television and medical image processing. From 1993 to 1998, he was with Philips Research Labs, Aachen, Germany, where he was responsible for several projects in X-Ray imaging and processing. In 1996, he was also an independent lecturer with the University of Magdeburg, Germany. In 1998, he was appointed a full professor and director of the Institute for Signal Processing, University of Luebeck. Since 2004, he has been Head of the Chair for Image Processing, Aachen University of Technology (RWTH). His research interests are in medical and industrial image processing, signal processing, pattern recognition, and computer vision. He is a Senior member of IEEE, an Associate Editor of the IEEE Transactions on Image Processing, and was Technical Program Co-Chair for the IEEE Southwest Symposium on Image Analysis and Interpretation (SSIAI) in 2000, 2002 and 2004.